



A Large Magnetic Hump in the VLISM Observed by Voyager 1 in 2020–2022

L. F. Burlaga¹, N. Pogorelov², L. K. Jian³, J. Park⁴, A. Szabo³, and N. F. Ness⁵¹Leonard F. Burlaga, Inc., Davidsonville, MD 21035, USA; lburlagahsp@verizon.net²University of Alabama in Huntsville, Huntsville, AL 35899, USA³Heliophysics Science Division, NASA/GSFC, Greenbelt, MD 20771, USA⁴University of Maryland, Baltimore County, Baltimore, MD 21250, USA⁵Independent scholar, Landenberg, PA 19350-9350, USA

Received 2023 January 14; revised 2023 May 17; accepted 2023 May 17; published 2023 August 10

Abstract

Voyager 1 has been moving through the very local interstellar medium (VLISM) for approximately one solar cycle, from 122.58 au on 2012/DOY 238 (August 25) to 158.5 au on 2023.0. Previously, an abrupt increase (“jump”) in the magnetic field strength B and proton density N by a factor of 1.35 and 1.36, respectively, was observed during an interval of ~ 8 days in 2020.40. After the jump, B continued to increase to a maximum value ~ 0.56 nT at ~ 2021.4 and then declined until B returned to the postjump value of 0.5 nT on 2021.85, 1.45 yr after the jump. The magnetic field strength declined briefly from 0.5 nT on 2021.85 to 0.47 nT on 2021.95 and then increased sporadically to 0.52 nT at 2023.0. Thus, the magnetic field strength remained strong for at least 2.6 yr. The magnetic hump and the density hump were a compression wave propagating through the VLISM. The compression wave was generated by a region with large dynamic pressure in the solar wind that propagated through the inner heliosheath and collided with the heliopause. The magnetic field strength continued to remain strong, with slow variations, until the end of our observations at 2023.0. It is suggested that the magnetic hump evolved from the large dynamic pressure, high speeds, and density observed at 1 au between ~ 2015 and ~ 2017 .

Unified Astronomy Thesaurus concepts: [Interstellar magnetic fields \(845\)](#)

1. Introduction

Voyager 1 was launched in 1977 and has been making observations during the last 45 yr, for more than four solar cycles, out to 158.5 au. The spacecraft moved beyond the planets, through the heliosphere, across the termination shock, through the heliosheath, and across the heliopause on 2012 August 25 and it has been moving through the interstellar medium for the last ~ 11 yr, which is nearly one solar cycle (Burlaga et al. 2013, 2019a; Krimigis et al. 2013, 2019; Stone et al. 2013, 2019; Gurnett & Kurth 2019; Richardson et al. 2019; Gurnett et al. 2021). The heliopause is the boundary of the heliosphere (Parker 1963; Zank 2015; Pogorelov et al. 2017, 2021) between the hot (10^5 – 10^6 K; McComas et al. 2011) plasma flowing outward from the Sun and the relatively cold (10^4 K; Frisch et al. 2011) plasma in the very local interstellar medium (VLISM). This paper discusses the magnetic field observations made by Voyager 1 in the VLISM. The instrument and methods for processing the data are described by Behannon et al. (1977) and Berdichevsky (2009, 2015).

Both Voyager 1 and Voyager 2 data show that the shocks observed in the VLISM are very much different from those detected in the solar wind. This is not surprising, because the solar wind plasma is collisionless beyond 1 au, but the VLISM is known to be collisional (Baranov & Ruderman 2013; Zank 2015). Voyager 1 observed two collisional shocks and at least one thick pressure front before 2020.

These events, which are plotted in Figure 1, have the form of (1) an abrupt increase (“jump”) in the magnetic field strength B

followed by (2) a very slow, nearly monotonic decrease in B . Such decreases are not surprising because the global trend for B is to decrease while it is undrapping toward its strength in the unperturbed VLISM. Since these events are discussed in detail by Burlaga et al. (2020a) and Burlaga et al. (2021), we briefly discuss the important points.

The first jump in B was observed by Voyager 1 shortly after crossing the heliopause, near 2012.92 (DOY 335), with a jump in the magnetic field $B_2/B_1 = 1.43$ and a proton density jump $N_2/N_1 = 1.36$. This event was identified as a shock (sh1), because it was preceded by electron plasma oscillation events as predicted by Gurnett et al. (1993) and Whang & Burlaga (1993, 1995). The electron density was $N_e = 0.05$ cm⁻³ (Gurnett et al. 2013), giving the first conclusive evidence that Voyager 1 entered the dense interstellar medium. The last day during which electron plasma oscillations were observed was 2012/DOY 332, near the shock on 2012/DOY 335. The time interval during which the jump in B moved past Voyager 1 was 4 days, which is the order of 10^4 times larger (approximately 0.12 au) than that expected.

Mostafavi & Zank (2018a, 2018b) and Mostafavi et al. (2022) showed that shock waves in the dense VLISM should have a dissipative structure defined by thermal conduction, the length scale for which is ~ 0.115 au for a plasma temperature of 7500 K. The viscous length scale for that temperature was estimated to be 0.03 au. However, Fraternali et al. (2020) and Fraternali & Pogorelov (2021) showed that the Coulomb mean free path can be as large as 2–4 au for a more realistic temperature of 30,000 K (Richardson et al. 2019). Pogorelov et al. (2021) suggested that the difference in thickness of observed shocks and pressure fronts is possibly indicative of the absence of a steady dissipative structure in all of these objects propagating through the evolving local interstellar medium (LISM). A second shock (sh2) was observed by

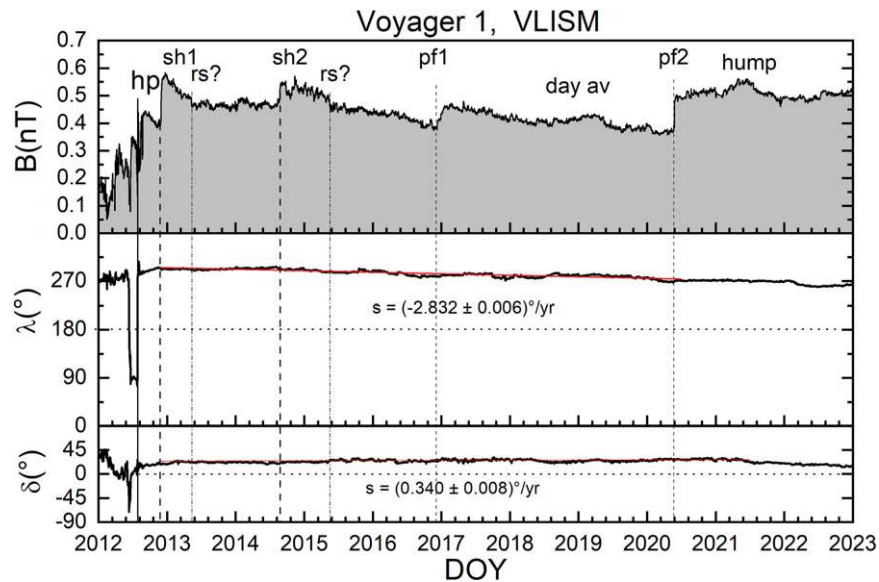


Figure 1. Observations of the magnetic field strength B , azimuthal angle λ , and elevation angle δ . The heliopause hp, shocks sh1 and sh2, and a pressure front pf1, each followed by a slow decay, and downward jumps (reverse shock?) that might evolve into reverse shocks are superimposed on a gradual decrease in B with increasing distance from the Sun or heliopause, until the arrival of the pressure front pf2 and the magnetic hump with strong magnetic fields throughout. The azimuthal angle λ and elevation angle δ vary nearly linearly with increasing time and distance. There may be a small decrease in δ following the maximum of the magnetic hump.

Voyager 1 on 2014.6438 (2014/DOY 236; Burlaga & Ness 2016). This shock moved past Voyager 1 in 3.3 days, and the ratio of $B_2/B_1 = 0.54 \text{ nT} / 0.48 \text{ nT} = 1.13$. This shock was also preceded by an interval containing electron plasma oscillations driven by electrons accelerated by a shock. Fraternali et al. (2020) showed that the shock sh2 was associated with weak intermittency in B . The motion of shocks through the VLISM was discussed by Kim et al. (2017).

The third event was distinctly different than the first two events. Beginning on 2016/DOY ≈ 346 , a jump in $B = 1.19$ moved past Voyager 1 in ~ 35 days, nearly 1 order of magnitude greater than the passage time of the shocks discussed above (Burlaga et al. 2019a). Burlaga et al. (2019b) identified the event as a pressure front, “pf1.”

The shocks sh1, sh2, and the pressure front pf1 were followed by a slow monotonic decrease of B to a plateau. In the fourth event, the jump in B called pf2 was followed by an increase in B (Burlaga et al. 2021). We shall show that B increased to a maximum and then slowly decreased to a value that was still higher than the prejump value observed 1.6 yr earlier. We shall call the strong magnetic fields following the jump during this extended interval “the magnetic hump.”

2. The Magnetic Hump

The fourth major jump in B , the “2020 event,” was observed by Voyager 1, beginning near 2020/DOY 147 in the magnetic field in the VLISM. The jump in B associated with this event was discussed by Burlaga et al. (2021), who showed that it was associated with the arrival of the magnetic hump pf2 with $B_2/B_1 = 0.46 \text{ nT} / 0.34 \text{ nT} = 1.35$. This jump was accompanied by a similar jump in the density, $N_2/N_1 = 1.36$. Burlaga et al. (2021) labeled the jump associated with the magnetic hump pf2 because, like the pressure front pf1, it was not accompanied by intense electron plasma oscillations, enhanced turbulence activity (Fraternali et al. 2020), or increased energetic particle intensities (S.M. Krimigis 2021, private communication; J.

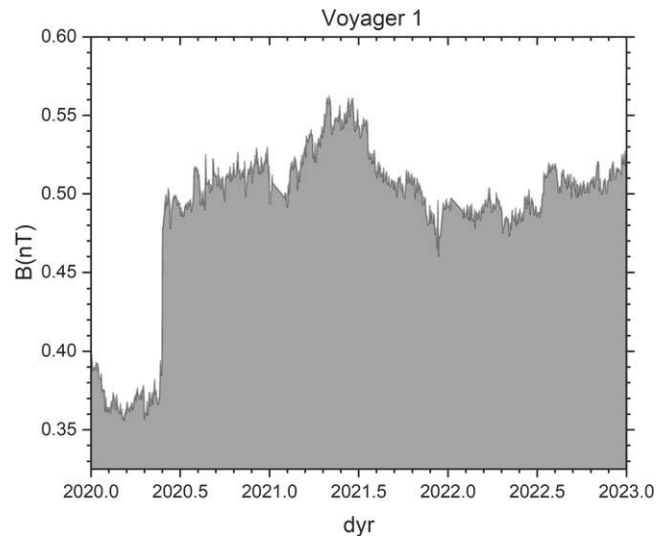


Figure 2. The magnetic hump. Increasing magnetic field strength to a maximum followed by a decrease to the postjump level was observed following pf2. The strong magnetic fields persisted for 2.6 yr.

Rankin 2022, private communication), which suggests that the jump in B near day 2020/146.90 may not be a shock.

However, the passage time of pf2 was less than 8 days, whereas the passage time of the pressure front pf1 was 32 days. In fact, the passage time of pf2 was not much longer than the passage time of the shocks discussed above, namely 5.4 and 3.3 days. Thus, the nature of pf2 is not understood. In particular, the possibility that pf2 was evolving to a shock cannot be excluded.

The magnetic field strength observed preceding the jump, the jump itself (pf2), and the magnetic hump are shown in Figure 1 where they can be compared with the other jumps discussed above. A high-resolution plot of the magnetic field strength in the magnetic hump is shown in Figure 2. The jump and the increasing magnetic fields were identified and discussed by

Burlaga et al. (2021). A further increase in the magnetic field of the magnetic hump to relatively high values until 2021.5 was discussed by Burlaga et al. (2022). Quasiperiodic variations with a period of approximately 30 days were observed during part of this increase, and it was suggested that these might be related to the rotation of the Sun and features on the Sun.

This paper (Figure 2) shows that the total increase to the maximum of B at 2020.4 was from 0.37 to 0.50 nT, an increase of ~ 0.13 nT. The maximum magnetic field strength was ~ 0.56 nT and occurred at ~ 2021.4 . The magnetic field then decreased back to the postjump level 0.5 nT on 2021.85. Thus, the magnetic field in the magnetic hump returned to its postjump level in 1.45 yr. Clearly, the magnetic hump defined in this way was a large feature. The magnetic field strength declined briefly from 0.5 nT on 2021.85 to 0.47 nT on 2021.95 (well above the prejump level 0.31 nT) and then increased sporadically to 0.52 nT at 2023.0. In other words, the magnetic field increased from 0.50 nT following the jump to ~ 0.56 nT at the peak of the hump and ended on 2023 (the extent of our observations) with $B \sim 0.52$ nT, which is the postjump level. Thus, the magnetic field strength remained strong for at least 2.6 yr.

The extensive magnetic hump in the VLISM, with its strong fields, was not predicted and it is still not understood. Recall that each of the three previous jumps was followed by a slowly *decreasing* field strength, which was superimposed on the long-term decrease in B . Thus, the magnetic hump is a new feature of the VLISM that has not been observed previously, even though Voyager 1 has been moving through the VLISM for nearly 1 solar cycle (nominally ~ 11 yr).

The average azimuthal angle λ observed by Voyager 1 during 2020–2022 was $271^\circ \pm 2^\circ$, and the average elevation angle was $\delta = 26^\circ \pm 3^\circ$, as shown in Figure 1. The slope of the azimuthal angle as a function of time was $(-2.832 \pm 0.006)^\circ \text{ yr}^{-1}$, and the slope of elevation angle was $(0.340 \pm 0.008)^\circ \text{ yr}^{-1}$ from 2020 through 2021. The azimuthal angle and elevation angle did not change significantly by more than 2° across pf2. In fact, these angles were nearly constant, from 2020.0 to 2023.0. The observations are consistent with the very small linear variation of the magnetic field direction that was observed throughout the VLISM, including the magnetic hump. Thus, this result is also consistent with a solar origin of the magnetic hump.

The most striking feature of the magnetic hump is that the strong magnetic fields were observed for at least 2.6 yr (Figure 2). The *increase* in values of B following the jump was in contrast to the *decrease* in values of B observed behind the shocks sh1 and sh2 and the pressure front pf1 shown in Figure 1 and discussed by Burlaga et al. (2022). The extensive region containing the magnetic hump is unlike anything observed previously in the VLISM.

What was the cause of the long-lasting strong magnetic fields in the magnetic hump observed by Voyager 1? The uniqueness of such behavior suggests that it may be related to some time-dependent phenomena that occurred within the solar cycle. Since the global trend in the distribution B with distance is its decrease with heliocentric distance, the opposite behavior is possible only if the solar wind conditions at 1 au, e.g., an increase in its ram pressure, create a prolonged interval of enhanced interstellar magnetic field strength.

Figure 3 shows the temporal variations from 2007 to 2023 of the following quantities measured near Earth, from top to bottom: (1) the sunspot number at 1 au, the magnetic field

strength (B), solar wind speed (V), the density (N), the dynamic pressure (pdyn), and the tilt of the heliosphere current sheet (HCS). The density, speed, dynamic pressure, and magnetic field strength were very large between ~ 2015 and 2017, during the declining phase of the solar cycle. The propagation time of the solar wind to the heliopause was ~ 1 yr, and the propagation time of the disturbances through the VLISM was ~ 4 yr (Kurth et al. 2023). We suggest that the magnetic hump was produced by a region of exceptionally large dynamic pressure observed near Earth between ~ 2015 and ~ 2017 , which moved through the solar wind and collided with the heliopause, thereby generating a strong compression wave in the VLISM. The compression wave was observed by Voyager 1 as the magnetic hump and a comparable long-duration increase in density (Kurth et al. 2023).

Yet another explanation of the magnetic hump observed by Voyager 1 may be related directly to the solar cycle effects. i.e., the interaction of slow and fast solar wind (SW), analyzed by Pogorelov et al. (2009). In Figure 4, we show the distribution of magnetic field, B , from that simulation in the meridional plane formed by the Sun’s rotation axis and the velocity vector in the uniform, unperturbed LISM. The range of values is chosen with a specific emphasis on the magnetic field distribution in the LISM. As seen from this figure, the maximum of B is on the heliopause. However, once per solar cycle, a relatively wide region of enhanced B is seen farther in the outer heliosheath. This means that during such an interval of time, Voyager 1 should measure a relatively large value of B after it is overtaken by an outward propagating shock. While the simulations in Pogorelov et al. (2009) represent the consequences of a nominal, self-repeating, 11 yr solar cycle with the variable latitudinal extent of the slow wind and the angle between the Sun’s rotation and magnetic axes, they still reproduce the global features of the flow qualitatively. Driven by the Ulysses data, the solar cycle simulations of Pogorelov et al. (2013) demonstrate very similar features.

3. Summary and Discussion

Voyager 1 crossed the heliopause on 2012 August 25 (Burlaga et al. 2013, 2019a) and it has been moving through the VLISM for 10 yr, nearly one solar cycle. Figures 1 and 2 of this paper show a new feature in the VLISM, the magnetic hump, in which the B *increased and remained high* for at least 2.6 yr. This feature was probably of solar origin. It was not observed during the first 9 yr that Voyager 1 moved through the VLISM, because the magnetic hump is observed only once in a solar cycle. Regardless of the origin and formation of the magnetic hump, we have shown that it exists in the VLISM and that it moved past Voyager 1 for at least 2.6 yr. It was accompanied by a “hump” in the density (Kurth et al. 2023). Together, the magnetic hump and the density hump constitute a compression wave that propagated through the large-scale boundary layer of the VLISM.

The magnetic hump was preceded by what was called a pressure front, pf2, by Burlaga et al. (2022), because it was not associated with a shock, electron plasma oscillations, or energetic particles. On the other hand, this paper shows that the magnetic hump was preceded by a jump in B that moved past the spacecraft in less than 8 days. This timescale is not much larger than that associated with two shocks, sh1 and sh2, for which the passage times were 5.4 days and 3.3 days, respectively. The passage times associated with the shocks

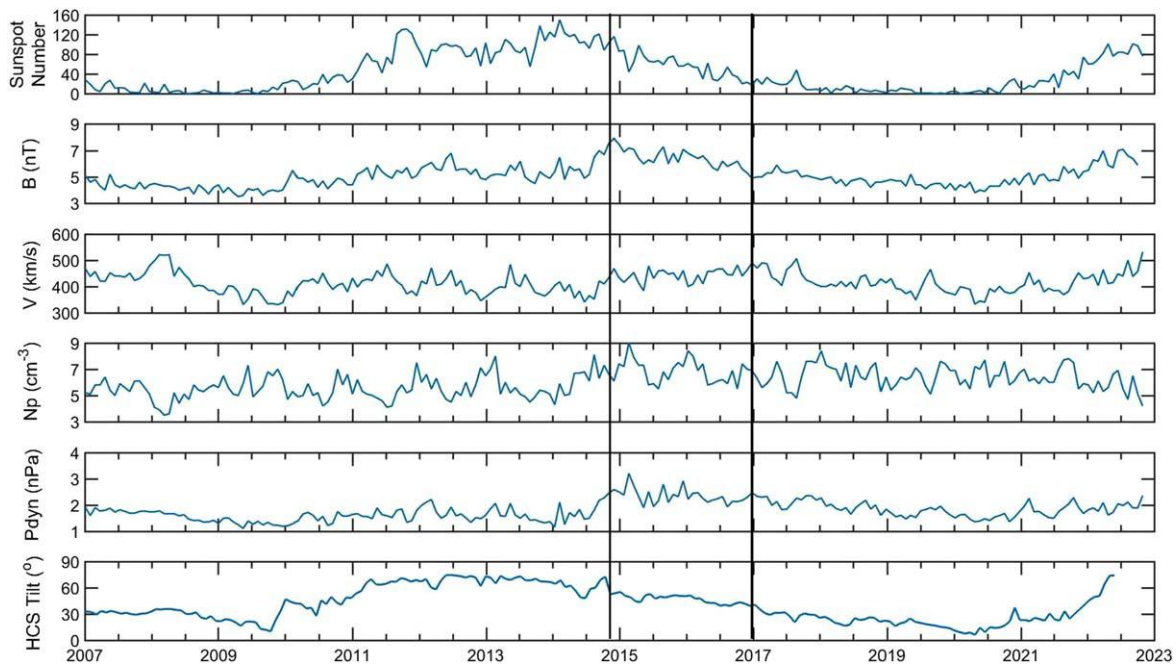


Figure 3. Solar and solar wind parameters that might be relevant to the formation and observation of the magnetic hump in the compression wave in the VLISM. From top to bottom are 27 day averages of sunspot number, the interplanetary magnetic field strength B , solar wind speed V , solar wind proton density N_p , dynamic pressure, and the tilt of the heliosphere current sheet (HCS). It is estimated that the propagation time from 1 au, through the solar wind, heliosheath, and VLISM to the time of the jump pf2 (~ 2020.4) was ~ 5 yr.

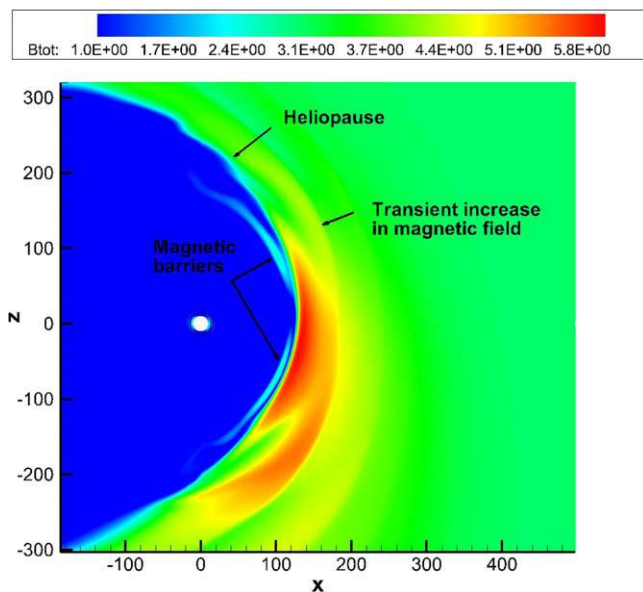


Figure 4. This figure shows the heliopause, the magnetic barriers following it, the compression ahead of the nose, as well as a transient increase in the magnetic field extending over a wide range of latitudes. This is a schematic illustration of what the magnetic hump might look like qualitatively.

were much shorter than the 32 days passage time of the pressure front pf1. Thus, we should not dismiss the possibility that the magnetic hump and the associated compressional wave were related to an MHD shock at some intervals in time. We have shown that an extended increase in the SW dynamic pressure can produce such a feature.

In addition, the solar cycle simulations in Pogorelov et al. (2009, 2013) support the existence of rather wide regions of enhanced magnetic field in the distant VLISM, which are

consistent with the observed hump. Continued observations and more detailed physical models are needed to explain the extent and origin of the magnetic hump.

ORCID iDs

L. F. Burlaga <https://orcid.org/0000-0002-5569-1553>
 N. Pogorelov <https://orcid.org/0000-0002-6409-2392>
 L. K. Jian <https://orcid.org/0000-0002-6849-5527>
 J. Park <https://orcid.org/0000-0002-8989-4631>
 A. Szabo <https://orcid.org/0000-0003-3255-9071>

References

- Behannon, K. W., Acuna, M. H., & Burlaga, L. F. 1977, *SSRv*, **21**, 235
 Baranov, V. P., & Ruderman, M. S. 2013, *MNRAS*, **434**, 3202
 Berdichevsky, D. B. 2015, Voyager Mission, Detailed Processing of Weak Magnetic Fields; II—Update on the Cleaning of Voyager Magnetic Field Density B with MAGCALs, version 11/7/2015
 Berdichevsky, D. B. 2009, White Paper, Voyager Mission, Detailed Processing of Weak Magnetic Fields I—Constraints to the uncertainties of the Calibrated Magnetic Field Signal in the Voyager Missions, https://spdf.gsfc.nasa.gov/pub/data/voyager/documents/vgsmag_website/Berdichevsky-VOY_sensor_opu090518.pdf
 Burlaga, L. F., Kurth, W. S., & Gurnett, D. A. 2021, *ApJ*, **911**, 61
 Burlaga, L. F., & Ness, N. F. 2016, *ApJ*, **829**, 134
 Burlaga, L. F., Ness, N. F., Berdichevsky, D. B., et al. 2019a, *NatAs*, **3**, 1007
 Burlaga, L. F., Ness, N. F., Berdichevsky, D. B., et al. 2019b, *ApJ*, **877**, 31
 Burlaga, L. F., Ness, N. F., Berdichevsky, D. B., et al. 2020a, *AJ*, **160**, 40
 Burlaga, L. F., Ness, N. F., & Berdichevsky, D. B. 2022, *ApJ*, **932**, 59
 Burlaga, L. F., Ness, N. F., Gurnett, D. A., & Kurth, W. S. 2013, *ApJL*, **778**, L3
 Fraternali, F., & Pogorelov, N. P. 2021, *ApJ*, **906**, 75
 Fraternali, F., Pogorelov, N., & Burlaga, L. F. 2020, *ApJL*, **897**, L28
 Frisch, P., Redfield, S., & Slaven, J. 2011, *ARA&A*, **49**, 237
 Gurnett, D. A., & Kurth, W. S. 2019, *NatAs*, **3**, 1024
 Gurnett, D. A., Kurth, W. S., Allendorff, S. C., & Poynter, R. L. 1993, *Sci*, **262**, 199
 Gurnett, D. A., Kurth, W. S., Burlaga, L. F., et al. 2021, *ApJ*, **921**, 62

- Gurnett, D. A., Kurth, W. S., Burlaga, L. F., & Ness, N. F. 2013, *Sci*, **341**, 1489
- Kim, T. K., Pogorelov, N. V., & Burlaga, L. F. 2017, *ApJL*, **843**, L32
- Krimigis, S. M., Decker, R. B., Roelof, E. C., et al. 2013, *Sci*, **341**, 144
- Krimigis, S. M., Decker, R. B., Roelof, E. C., et al. 2019, *NatAs*, **3**, 997
- Kurth, W. S., Burlaga, L. F., Kim, T., Pogorelov, N. V., & Granroth, L. J. 2023, *ApJ*, in press
- McComas, D. J., Angold, N., Elliott, H. A., et al. 2011, *ApJ*, **779**, 2
- Mostafavi, P., & Zank, G. P. 2018a, *ApJL*, **854**, L15
- Mostafavi, P., & Zank, G. P. 2018b, *JPhCS*, **1100**, 012018
- Mostafavi, P., Burlaga, L. F., Cairns, I. H., et al. 2022, *SSRv*, **218**, 27
- Parker, E. 1963, *Interplanetary Dynamical Processes* (New York: Interscience)
- Pogorelov, N. V., Borovikov, S. N., Zank, G. P., & Ogino, T. 2009, *ApJ*, **696**, 1478
- Pogorelov, N. V., Fraternali, F., Kim, T. K., Burlaga, L. F., & Gurnett, D. A. 2021, *ApJL*, **917**, L20
- Pogorelov, N. V., Heerikhuisen, J., & Roytershteyn, V. 2017, *ApJ*, **845**, 9
- Pogorelov, N. V., Suess, S. T., Borovikov, S. N., et al. 2013, *ApJ*, **772**, 2
- Richardson, J., Belcher, J. W., Garcia-Galendo, P., & Burlaga, L. F. 2019, *NatAs*, **3**, 1019
- Stone, E. C., Cummings, A. C., Heikkila, B. C., & Lal, N. 2019, *NatAs*, **3**, 1013
- Stone, E. S., Cummings, A. C., McDonald, F. B., et al. 2013, *Sci*, **341**, 150
- Whang, Y. C., & Burlaga, L. F. 1993, *JGR*, **98**, 15221
- Whang, Y. C., & Burlaga, L. F. 1995, *JGR*, **100**, 17023
- Zank, G. P. 2015, *ARA&A*, **53**, 449